

H. -R. XIA, L. -X. LI, J. -Y. WANG, Y. -G. LIU, J. -Q. WEI

Department of Physics, Environmental Engineering Department, and National Laboratory of Crystal Materials, Shandong University, Jinan, People's Republic of China

Soft-Mode Spectroscopy in Fe:KTa_{1-x}Nb_xO₃ Crystals

Fe-doped potassium tantalite niobate, Fe:KTa_{1-x}Nb_xO₃ (Fe:KTN), crystallizes with $x = 0.48$ and a perovskite-type structure in tetragonal system with point group $4mm$, conforming space group $P4mm$. The paraelectric-ferroelectric structural transition of the Fe:KTN is studied by Raman scattering investigations. A condensed soft lattice vibrational mode at the phase transition has been analyzed. It originates from the symmetric O2/O3-Nb/Ta-O3/O2 in-plane bending of the Nb/TaO₆ group. The soft optical phonon mode concerns the extraordinary transverse optical phonons propagating along the $[1\bar{1}0]$ direction. The Raman spectra measured reflect the crystal disorder. Curie temperature measured by two methods is within 353 and 356.5 K.

Keywords: structural phase transition, soft lattice vibrational mode, Raman scattering

(Received June 26, 2000; Accepted September 6, 2000)

Introduction

Fe-doped potassium tantalite niobate, Fe:KTa_{1-x}Nb_xO₃ (Fe:KTN), has large quadratic or linear electro-optic coefficients. During recent years their important applications in many field of nonlinear optics, such as photorefractive properties and self-pumped phase conjugation (LIAN et al., and WANG et al.), have stirred people's broad interest. The properties and phase transition temperatures of Fe:KTN vary in a wide range with their changed contents. When cooled from high temperature, they exhibit different phases in a sequence of cubic ($m\bar{3}m$)-tetragonal ($4mm$)-orthorhombic ($mm2$)-rhombohedral ($3m$). Before now the structure phase transitions, lattice dynamics and ferroelectric properties of niobates, tantalates, titanates, and their some solid solutions with the tetragonal perovskite-type structure at room temperature have been studied by both theory and experiments including neutron and Raman scattering and infrared reflectivity spectroscopy (SLATER, COCHRAN, COWLEY, TRIEBWASSER, HEWAT, LANZI et al., BARKER et al., and SPITZER et al.). However, the space group theoretical analyses and assignment of the soft lattice mode have not been made so far. In this paper, we report mainly the cubic-tetragonal phase transition and the soft-mode spectroscopy in Fe:KTN.

Experimental

The top-seeded solution growth (TSSG) has gradually won popularity recently in the growth of nonlinear crystals (ZHONG). Using TSSG, we have grown tetragonal perovskite Fe:KTN crystals, with its size as large as $35 \times 35 \times 18 \text{ mm}^3$. Atomic absorption analysis, using a 180-80 atomic spectrum absorptiometer with a precision of $< 0.1 \text{ ppm}$ for Fe atom, shows $x =$

0.48, indicating the paraelectric-ferroelectric phase transiting at 356.5 K (BUFFAT et al.). The crystal structure and lattice parameters were measured by a $R3m/E$ x-ray four-circle diffractometer with a precision of 0.1° at room temperature. The experimental results show the same diffraction peak position belonging to point group $4mm$, conforming to the space group $P4mm$, similar to the perovskite-type structure. The lattice parameters obtained by least-squares refinement were $a = b = 0.3995$ (3) and $c = 0.4062$ (2) nm. The primitive cell contains the one formula unit. Fe:KTN was cut into sample along the a -, b -, and c -axes, with the size of $6 \times 6 \times 8$ mm³, of a precision of $1'$. The sample optically polished has high optical quality, which allows the study of the optical properties. Raman spectra were measured on an SPEX-1403 Raman spectrometer with a slit width of 100 μ m, using a 300-mW argon ion laser at 514.5 nm with a power density of 1.8 W/cm² at the sample. The Raman spectra with a resolution of 0.15 cm⁻¹ and a wavelength precision of 1 cm⁻¹ in a frequency range from 20 to 1000 cm⁻¹ were collected three times.

Space group analysis

The structure of Fe:KTN is of tetragonal perovskite type with the space group $P4mm$, a symmorphic space group and hence the translation operator $t = T(0, 0, 0)$. The primitive cell contains the one formula unit. The reducible representations for the $P4mm$ space group at the center Γ point of the first Brillouin zone are given in Table 1, using the group theory and The International Table for Crystallography (HAHN).

Symmetry species of point group			E	$2C_4(z)$	C_2	$2\sigma_v$	$2\sigma_d$
4mm and its Seitz operator			$1[0] t$	$4[001] t$	$2[001] t$	$m[100] t$	$m[110] t$
Atom, Wyckoff	O2,O3	$2c$	6	0	-2	2	0
position, and	Nb/Ta,O1	$1b$	3	1	-1	1	1
character	K	$1a$	3	1	-1	1	1

Table 1: The reducible representations for $P4mm$ at Γ point.

Based on the factor group theory, the reducible representations shown in Table 1 can be reduced as

$$\begin{aligned} 2c: & 1A_1 + 1B_1 + 2E; \\ 1b: & 2A_1 + 2E; \\ 1a: & 1A_1 + 1E. \end{aligned}$$

According to the character table of the point group $4mm$, the Raman (R)- and infrared (IR)-active optical phonon modes at zero wave vector are

$$\Gamma_{\text{vib}} = 3A_1(R, \text{IR}) + 1B_1(R) + 4E(R, \text{IR}).$$

It is clear that there are no more than 12 and 7 theoretically observable Raman peaks and infrared reflection bands, respectively. The concerned Raman scattering tensors are (LOUDON)

$$A_1(Z): \begin{bmatrix} a & 0 & 0 \\ 0 & a & 0 \\ 0 & 0 & b \end{bmatrix}, B_1: \begin{bmatrix} c & 0 & 0 \\ 0 & -c & 0 \\ 0 & 0 & 0 \end{bmatrix}, E(X): \begin{bmatrix} 0 & 0 & e \\ 0 & 0 & 0 \\ e & 0 & 0 \end{bmatrix}, \text{ and } E(Y): \begin{bmatrix} 0 & 0 & 0 \\ 0 & 0 & e \\ 0 & e & 0 \end{bmatrix}.$$

The symmetry representations $A_1(Z)$, $E(X)$, and $E(Y)$ show dipole moments oriented along the Z -, X -, and Y -directions, respectively. Because of equivalence of the axes X and Y for the measurement of Raman spectra of uniaxial crystals with the point group $4mm$ (LIU et al.), the interesting scattering configurations are $X(ZZ)Y$, $X(YZ)Y$, and $X(YY)Z$, corresponding to the representations $A_1(Z)$, $E(X/Y)$, and $A_1(Z)+B_1$, respectively. For the $X(YY)Z$, the symmetry species of the extraordinary phonons is undefined because the angle included between the phonon wave vector and the optical axis is 45° , which is most favorable for observing the directional dispersion of the extraordinary phonons (MERTEN). We have seen that the lattice vibrational spectra of the octahedral $(\text{NbO}_6)^{7-}$ -ion in some crystals, such as the tungsten bronze (TB)-type and LiNbO_3 crystals (XIA et al., BOUDOU et al., and SCHAUFLELE et al.), are similar to each other and show a common characteristic. An octahedral molecule XY_6 with the symmetry O_h has 15 internal vibrational degrees of freedom or six normal vibrational modes ν_i as shown in Fig. 1. They can be represented from group theoretical consideration as (XIA et al.)

$$\Gamma_{\text{vib}}' = A_{1g}(\nu_1, R) + E_g(\nu_2, R) + T_{1u}(\nu_3, \text{IR}) + T_{1u}(\nu_4, \text{IR}) + T_{2g}(\nu_5, R) + T_{2u}(\nu_6, \text{Inactive}),$$

where the subscripts g and u represent symmetric and antisymmetric vibrations, respectively. The ν_1 , ν_2 , and ν_3 are all stretch vibration modes, and the ν_4 , ν_5 , and ν_6 are all bend vibration modes. From a crystallographic viewpoint, the Fe:KTN crystal should also have the three characteristic Raman peaks and two strong characteristic infrared reflection bands as the internal vibrational modes of the octahedral $(\text{Nb/TaO}_6)^{7-}$ -ion in Fe:KTN to be observed and measured. Thus the three Raman-active vibrational modes imply a non-degenerate symmetric X - Y stretching $A_{1g}(\nu_1)$, a doubly degenerate symmetric Y - X - Y stretching $E_g(\nu_2)$, and a triply degenerate symmetric Y - X - Y bending $T_{2g}(\nu_5)$.

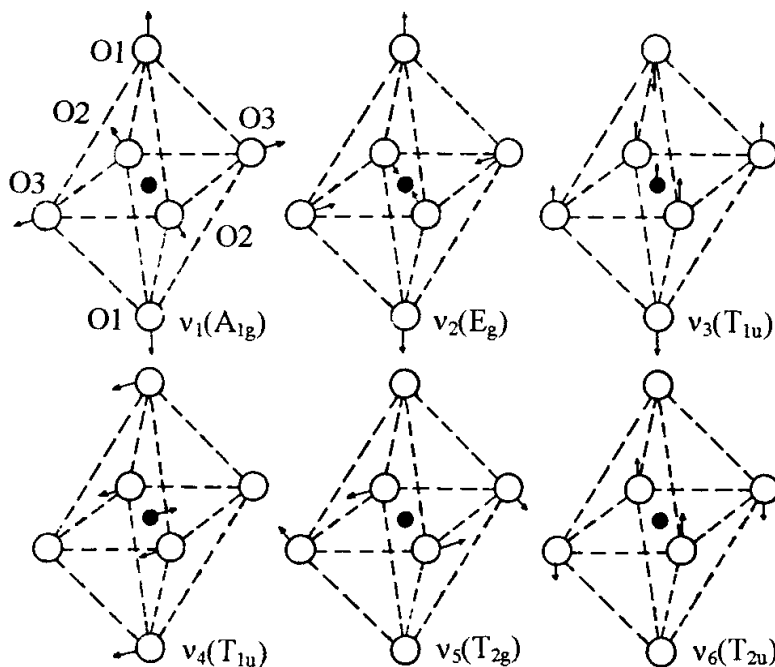


Fig. 1: Normal vibrational modes of an octahedral molecule XY_6 with O_h symmetry.

Result and discussion

Figure 2 shows the typical Raman spectra of the crystals with the octahedral ions, recorded in Fe:KTN at room temperature in a frequency range from 20 to 1000 cm^{-1} . The spectrum (a) in Fig. 2 corresponds to the symmetry species $A_1(Z)$ with the scattering geometry $X(ZZ)Y$, concerning extraordinary transverse optical phonons propagating along the $[1\bar{1}0]$ direction. Compared with the Raman spectra of the NbO_6 group in the TB-type crystals measured under same conditions (XIA et al.), it is easy to determine the two of the three internal vibrational modes of the Nb/TaO_6 group in Fe:KTN to be 875(ν_1) and 556(ν_2) cm^{-1} . The third (ν_3) have been split into 160/180/205 cm^{-1} for there are the comparatively rigid oxygen octahedra distorted in the $4mm$ phase and deviation from O_h symmetry will result in line broadening or even splitting. Perhaps the broadening or splitting has occurred also due to the partially substituting the Ta^{5+} ion for the Nb^{5+} ion. The spectrum (b) in Fig. 2 corresponds to the $E(X/Y)$ symmetry species with the $X(YZ)Y$ scattering configuration, which involves ordinary transverse and extraordinary longitudinal optical phonons propagating along the $[1\bar{1}0]$ direction. The four Raman peaks of 827, 542, 275, and 196 cm^{-1} are all doubly degenerate. In Fig. 2 compared the spectrum (c) with the spectrum (a), the mode ν_1 in the spectrum (c) is 871 cm^{-1} . The peak of 108 cm^{-1} should belong to the species B_1 , a nonpolar mode, and is the external lattice vibrational mode for the Nb/TaO_6 group. The ν_2 mode has been split into 472/568 cm^{-1} . The ν_3 mode has disappeared.

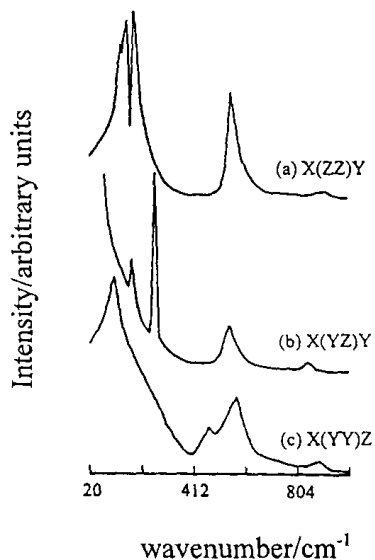


Fig. 2: Raman spectra recorded in Fe:KTN at 298 K between 20 and 1000 cm^{-1} .

In Fig. 2, in the spectrum (a) the Raman lines are too many by two than that of the factor group analysis; in the spectrum (b) the count background at the low wave number increases largely; and in the spectrum (c) the mode ν_2 was split and the mode ν_3 disappeared. These imply the disorder of Fe:KTN crystal, which is due to the crystal defects and/or dopant and affects the selection rule of Raman scattering (LANZI et al.). Also, the state of the spectrum (c) in Fig. 2 is due to the directional dispersion of the extraordinary phonons.

The sample was heated slowly up to 128 $^{\circ}\text{C}$, then the drop-temperature Raman spectra were measured to study the $m\bar{3}m$ - $4mm$ phase transition and the soft lattice vibrational mode.

Figure 3 shows three sets of the Raman lines around the ν_1 , ν_2 , and ν_5 versus temperature from 128 to 28 °C, recorded in Fe:KTN with the scattering geometry $X(\bar{Z}Z)Y$ belonging to the $A_1(Z)$, an all-symmetry species. As seen, the phase transition temperature is about 80 °C. The mode ν_5 is a soft lattice vibrational mode according to Cochran's soft mode theory (COCHRAN). The phase transition is first order for Fe:KTN by means of Triebwasser's conclusion (TRIEBWASSER). As in Pytte's work (PYTTE), the soft lattice mode at the paraelectric phase is triply degenerate.

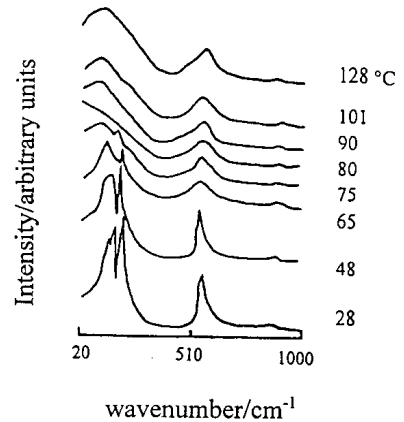


Fig 3: Three sets of Raman lines around ν_1 , ν_3 , and ν_5 vs temperature from 128 to 28 °C, recorded in the Fe:KTN with the scattering geometry $X(\bar{Z}Z)Y$.

For a rigid Nb/Ta-O octahedron with the symmetry O_h in Fe:KTN crystal, the mode ν_5 shows a triply degenerate symmetric O2/O3-Nb/Ta-O3/O2 in-plane bending (deformation or scissor) vibration. When the paraelectric-ferroelectric phase transition occurs, the displacing of the O2 and O3 atoms on the equatorial plane of the octahedron is not synchronous owing to the thermal fluctuations. Thus the octahedra deviate from the O_h symmetry, and the mode ν_5 also deviates from the symmetric bending vibration and approximately approaches to the antisymmetric bending vibration; i.e., the mode ν_6 of the Raman- and infrared-inactive, a die mode. At the stable $4mm$ phase, the Nb/Ta atoms have deviated from the equatorial plane along the c -axis, and the mode ν_5 should be broadened or split. Of course, the modes ν_1 and ν_2 should also be broadened and the ν_2 would be evenly split, also due to no symmetric displacements of the two axial O1 atoms along the c -axis. Even though the displacive phase transition occurs, the modes ν_1 and ν_2 are not also condensed as the soft lattice vibrational modes because they are all symmetric stretching vibrations. It may be seen that there is only a soft lattice vibrational mode ν_5 , that is to say, the condensed soft optical phonon mode is from the symmetric O2/O3-Nb/Ta-O3/O2 in-plane bending vibration at the cubic-tetragonal ferroelectric structural transition of Fe:KTN. The structural rigidity is mainly ascribed to the symmetric Nb/Ta-O and O-Nb/Ta-O stretching vibrations (modes ν_1 and ν_2) as well as to the antisymmetric Nb/Ta-O stretching and O-Nb/Ta-O in-plane bending vibrations (modes ν_3 and ν_4). Because there is no polar external vibrational mode, the structural rigidity has little relation with the potassium-oxygen interactions.

Conclusion

The paraelectric-ferroelectric structural transition of the tetragonal perovskite-type Fe:KTN crystal with the T_c within 353 and 356.5 K is the first order. Only a condensed soft optical phonon mode ν_5 concerns the extraordinary transverse optical phonons propagating along the

[110] direction. At the paraelectric phase $m\bar{3}m$, the mode ν_5 is triply degenerate, originating from the symmetric O2/O3-Nb/Ta-O3/O2 in-plane deformation vibration of the rigid Nb/TaO₆ group with the symmetry O_h . At the room-temperature ferroelectric phase $4mm$, the mode ν_5 is split into the three Raman lines due to the distortion of the comparatively rigid Nb/TaO₆ group deviating from the O_h symmetry. The structural rigidity is mainly ascribed to the symmetric Nb/Ta-O and O-Nb/Ta-O stretching vibrations as well as to the antisymmetric Nb/Ta-O stretching and O-Nb/Ta-O in-plane bending vibrations.

Acknowledgments

National Natural Science Fund and Shandong Provincial Natural Science Fund support this work. It is also supported by a grant for State Key Program, and by National Laboratory of Crystal Materials of Shandong University, China.

References

- BARKER, A. S., Jr. and TINKHAM, M.: Phys. Rev. **125** (1962) 1527
 BOUDOU, A., SAPIRIEL, J.: Phys. Rev. B **21** (1980) 61
 BUFFAT, Ph., GANIERE, D., RAPPAZ, M., RYTZ, D.: J. Cryst. Growth **74** (1986) 353
 COCHRAN, W.: Adv. Phys. **9** (1960) 387
 COWLEY, R. A.: Phys. Rev. **134** (1964) A981
 HAHN, T.: *International Tables for Crystallography*, Vol. A: *Space-Group Symmetry*, PP. 506-509. Reidel, Dordrecht (1983)
 HEWAT, A. W.: J. Phys. C: Solid State Phys. **6** (1973) 1074 and 2559
 LANZI, G., MILANI, P., SAMOGGIA, G., MAGLIONE, M., HOCHLI, U. T.: Phys. Rev. B **36** (1987) 1233
 LIAN, Y., GAO, H., YE, P., GUAN, Q., WANG, J.: Appl. Phys. Lett. **63** (1993) 1745
 LIU, S. M., ZHANG, G. Y.: Acta Phys. Sinica **32** (1983) 657 (in Chinese)
 LOUDON, R.: Adv. Phys. **13** (1964) 423; errata: Adv. Phys. **14** (1965) 621
 MERTEN, L.: Z. Naturforschung **22a** (1967) 359
 PYTTE, E.: Phys. Rev. **B5** (1972) 3758
 SCHAUFLE, R. F., WEBER, M. J.: Phys. Rev. **152** (1966) 705
 SLATER, J. C.: Phys. Rev. **78** (1950) 748
 SPITZER, W. G., MILLER, R. C., KLEINMAN, D. A., HOWARTH, L. E.: Phys. Rev. **126** (1962) 1710
 TRIEBWASSER, S.: Phys. Rev. **114** (1959) 63
 WANG, J., GUAN, Q., LIU, Y., WEI, J., WANG, D., LIAN, Y., YANG, H., YE, P.: Appl. Phys. Lett. **61** (1992) 2761
 XIA, H. R., CHEN, H. C., YU, H., HU, L. J., WANG, K. X., ZHAO, B. Y.: Phys. Rev. B **54** (1996) 8954
 XIA, H. R., WANG, C. J., YU, H., CHEN, H. C., WANG, M.: J. Appl. Phys. **82** (1997) 4465
 XIA, H. R., YU, H., YANG, H., WANG, K. X., ZHAO, B. Y., WEI, J. Q., WANG, J. Y., LIU, Y. G.: Phys. Rev. B **55** (1997) 14 892
 ZHONG, S. D.: Progr. Cryst. Growth Charact. **20** (1990) 161

Contact information:

Prof. HAI-RUI XIA*
 Department of Physics, Shandong University
 Jinan 250100, People's Republic of China

Ms. LI-XIA LI
 Environmental Engineering Department, Shandong University
 Jinan 250100, People's Republic of China

Prof. JI-YANG WANG, Prof. YAO-GANG LIU, Prof. JING-Qian WEI
 National Laboratory of Crystal Materials, Shandong University
 Jinan 250100, People's Republic of China

*corresponding author: e-mail: hrxia@sdu.edu.cn